ELSEVIER

Carbohydrate Research 303 (1997) 379–393

CARBOHYDRATE RESEARCH

Dynamic behavior of a perfunctionalized β-cyclodextrin as probed by NMR and molecular modeling

Laurent Catoire [a], Veronique Michon [a], Laurence Monville [a], Alexandre Hocquet [a], Ludovic Jullien [a], Josette Canceill [b], Jean-Marie Lehn [b], Martial Piotto [c], Catherine Hervé du Penhoat [a,*]

[a] *Département de Chimie, URA 1679, Ecole Normale Supérieure, 24 rue Lhomond, F-75231 Paris, France*

[b] *Laboratoire de Chimie des Interactions Moléculaires, UPR 285, Collège de France, 11 Place Marcelin Berthelot, F-75231 Paris Cedex 05, France*

[c] *Unité Mixte de Recherche Bruker, CNRS, Université Louis Pasteur, UMR 50, F-67166 Wissembourg, France*

Received 4 April 1997; accepted 20 June 1997

Abstract

Conformational analysis of a perfunctionalized β-cyclodextrin by NMR and molecular modeling has revealed that this compound exists as an equilibrium mixture of C_1 and C_7 conformers in slow exchange. From carbon chemical shifts, interglycosidic vicinal heteronuclear coupling constants and NOESY volumes, it has been demonstrated that the macrocyclic conformation is responsable for the asymmetry in the C_1 form. Several dynamic processes such as rapid conformational averaging, localized chemical exchange and the C_1/C_7 equilibrium have been shown to occur on widely separated timescales. In parallel, a molecular modeling study has revealed that the accessible conformational space of β-CDs is not significantly reduced with respect to that of the related disaccharide, β-maltose. All of the dynamic phenomena appear to be related to the macrocylic puckering and two distinct modes of variation in puckering have emerged from MD trajectories: transitions are either auto-compensated without perceptible change in macrocycle puckering or irreversible leading to considerable variation in macrocycle puckering. Optimization of the NMR-defined theoretical structures leads to auto-complexation of an exocyclic substituent. © 1997 Elsevier Science Ltd.

Keywords: NMR; Molecular dynamics; Macrocyclic puckering

* Corresponding author.

0008-6215/97/$17.00 © 1997 Elsevier Science Ltd. All rights reserved.
PII S0008-6215(97)00188-2

1. Introduction

With the advent of supramolecular chemistry, considerable effort has been devoted to the synthesis and structural characterization of macrocyclic compounds over the past two decades. Such molecules often adopt structures which contain molecular cavities that can accommodate guest compounds. Although already analyzed in some detail (for reviews see [1,2]), the driving force governing host–guest interactions in such species is still poorly understood. It has been postulated that the presence of clefts in the empty host often causes the solvent to locally adopt high-energy configurations. The removal of the solvent from the cavity partially provides the driving force for guest complexation (solvophobic effect). In studies of the solution behaviour of cyclodextrin derivatives [3], the conformational preferences have been tentatively rationalized by focusing on the importance of hydroxyl substitution of the native cyclodextrins (lack of network of internal hydrogen bonds, steric hindrance,...). In fact, such explanations implicitly assume that the modification of the cyclodextrin sugar backbone during substitution does not alter significantly its Gibbs free energy. The present paper analyzes how far such an assumption may be considered as valid.

To address this issue, the structural characterization of the symmetrically modified β-cyclodextrin [4], **1** [per-2,3-di-*O*-benzyl-per-6-*O*-(2-methoxy)-(6-naphthoyl)-β-cyclodextrin], was undertaken with both NMR and molecular modeling methods. In earlier work [4], it was demonstrated that **1** (as well as many other perfunctionalized CDs) exists as a mixture of symmetrical and unsymmetrical conformers of similar stabilities in slow exchange at room temperature.

The major goals of this work were (i) to elucidate the nature of the conformational changes which lead to the loss of the seven-fold axis of symmetry and in particular to obtain direct evidence for a modification of the CD-backbone in the unsymmetrical conformer, (ii) to establish a motional model for the various types of conformational fluctuations with particular emphasis on the general case of symmetrical macrocyclic compounds [5,6] for which it is of interest to evaluate the length of the simulations required for reproducing the observed time-averaged molecular symmetry, (iii) to improve our understanding of the relationship existing between the molecular structure of derivatized CDs and their conformational behaviour with special emphasis on Gibbs free energies involved in the conformational equilibria and on the corresponding activation energies.

2. Experimental

Nomenclature.—The synthesis of per-2,3-di-*O*-benzyl-per-6-*O*-(2-methoxy)-(6-naphthoyl)-β-cyclodextrin, **1**, has been reported elsewhere [4]. A schematic representation of **1** is given in Fig. 1 along with the numbering of the heavy atoms and the protons of interest. The sign of the torsion angles is defined in agreement with the IUPAC-IUB Commission of Biochemical Nomenclature [7]. The notation used to define the conformation about the glycosidic linkage bonds is as follows:

Φ_H = H-1–C-1–O-4′–C-4′,

Ψ_H = C-1–O-4′–C-4′–H-4′,

β = C-1–O-4′–C-4′.

The puckering of the pyranosyl rings is defined by the ν_i dihedrals and that of the CD macrocycle is described by θ_L:

ν_1 = C-1–O-5–C-5–C-4,

ν_2 = O-5–C-5–C-4–C-3,

ν_3 = C-5–C-4–C-3–C-2,

ν_4 = C-4–C-3–C-2–C-1,

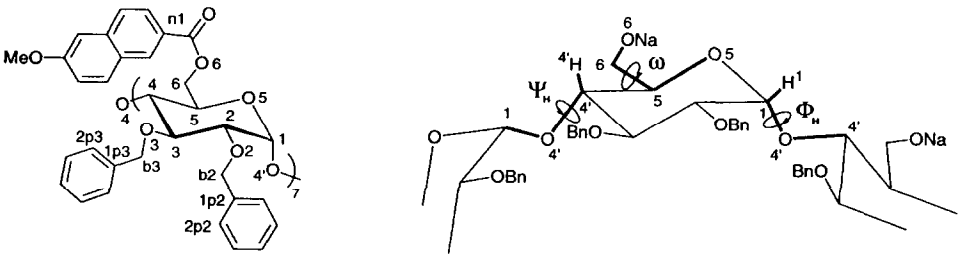

Fig. 1. (left) Molecular formula of modified β-cyclodextrin **1** with numbering of the heavy atoms. (right) Schematic representation illustrating the definition of several dihedral angles (Φ_H, Ψ_H, ω) involved in the conformational description of **1**.

ν_5 = C-3–C-2–C-1–O-5,

ν_6 = C-2–C-1–O-5–C-5,

and

θ_L = O-4–C-4–C-1–O-4′.

The orientation of the C-6 exocyclic group is as follows:

ω = O-5–C-5–C-6–O-6.

NMR Spectroscopy.—^{1}H (400.13, 500.13, and 750.13 MHz) and ^{13}C (100.6 and 188.63 MHz) spectra of a 10 mM solution of **1** in acetone-d_6 were recorded with Bruker instruments operating in the Fourier transform at 296 K unless stated otherwise. Tubes used in the relaxation experiments were degassed with five freeze–pump–thaw cycles under argon and then sealed. Chemical shifts for the pyranosyl and benzylic methylene protons were assigned from phase-sensitive COSYDQF and NOESY (2K × 2K data matrix; 3 Hz/pt) spectra, and a COSYLR (1K × 1K data matrix; 3 Hz/pt) experiment. Carbon chemical shifts for the pyranosyl and benzylic methylene carbons were assigned from the HETCOR spectrum. Vicinal coupling constants, $^3J_{H,H}$, were extracted from the 1D spectrum with a digital resolution of 0.12 Hz/pt where possible. In the other cases, the cross-peak patterns in the COSYDQF spectrum for a given type of coupling (i.e. H-1/H-2) were compared to those corresponding to a multiplet which was amenable to analysis in the 1D spectrum (vide infra). The mixing time for the 750.13 MHz NOESY spectrum was 200 ms. Quantitative 400.13 MHz phase-sensitive NOESY [8] spectra were acquired with mixing times of 0 and 400 ms. A 20 ms variable delay was introduced at the beginning of the mixing time in order to suppress *J*-peak transfer [9,10]. The recycle time was set to 5 times the longest T_1 in order to obtain a symmetrical normalized NOESY volume matrix. The diagonal (a_{kk}) and cross peak (a_{kl}) intensities were evaluated either from the summed F_1 subspectra contributing to a specific signal and/or with the volume integration routine in the commercial package Sybyl6.0 (Tripos Assoc.). Integration of noise in these spectra gave ±0.005 units of normalized intensity with respect to the diagonal volume (τ_m = 0 s) for typical peak widths.

^{13}C T_1 measurements were acquired with the inversion-recovery sequence (180–τ–90–FID) and relaxation times were calculated with the Bruker T_1 routine. The heteronuclear NOE factor (η) was established with the inverse-gated technique. Heteronuclear coupling constants were determined at 500.13 MHz with a ^{13}C-ω_1-half-filtered NOESY [11] experiment according to the following sequence:

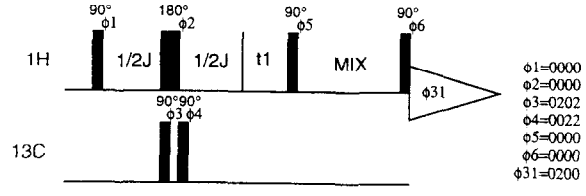

In the case of β-CD **1**, NOE mixing was necessary instead of TOCSY mixing since the scalar coupling between H-4′ and H-1 is negligible. The NOESY mixing time was set to 350 ms and the delay 1/2 J to 3.5 ms (141 Hz). All phases preceding the t1 evolution time were cycled through the TPPI procedure to achieve sign discrimination in F1 [12]. The sample concentration was roughly 20 mM and the total measuring time for the data matrix (2048 × 256 points, 9 and 1 Hz/pt in F1 and F2, respectively) was 48 h.

This experiment is based on the fact that if one selects a H-4′ proton bonded to a ^{13}C nucleus (1.1% of the molecules) during the first part of the sequence, this proton will precess under the influence of $^1J_{H\text{-}4',C\text{-}4'}$ (~ 140 Hz) during t1. Depending on the spin state of the ^{13}C nucleus (α or β) the proton will precess at its frequency ($\nu_{H\text{-}4'}$) minus ($^1J_{H\text{-}4',C\text{-}4'}$)/2 (α case) or plus ($^1J_{H\text{-}4',C\text{-}4'}$)/2 (β case). The NOE mixing process will then transfer the magnetisation from H-4′ to H-1. This proton is attached to a ^{12}C nucleus (98.9% of the molecules) and will therefore evolve during t2 under the influence of $^3J_{H\text{-}1,C\text{-}4'}$ (the coupling constant we want to measure). As the ^{13}C-4′ is still in the same spin state (α or β) as during t1, the H-1 proton will precess at its frequency ($\nu_{H\text{-}1}$) minus ($^3J_{H\text{-}1,C\text{-}4'}$)/2 (α case) or plus ($^3J_{H\text{-}1,C\text{-}4'}$)/2 (β case). This phenomenon gives rise to the pattern observed in such spectra [11].

Computational methods.—The absence of strong solvent effects on the position of conformational equilibria and corresponding activation energies [4] justifies in vacuo molecular modeling of this carbohydrate for which meaningful condensed-phase simulations would be unreasonably long (483 atoms). The in vacuo behavior of modified β-CD **1** and unmodified β-CD **2** was investigated using the carbohydrate force field developed by Ha et al. [13] (hereafter referred to as the HGFB force field). This force field was implemented in the general molecular mechanics CHARMm program and parameters for the aromatic atom types were taken from the general force field available in the CHARMm program [14]. The initial

coordinates for the cyclodextrin macrocycle **2** were those reported [15] for crystalline β-cyclodextrin ethanol octahydrate. Modified β-CD **1** was constructed with the molecular graphics software Quanta 4.0 (MSI Inc.) by progressively introducing the benzyl groups at the O-2 and O-3 positions followed by the naphthoyl moieties at O-6. The partial charges of the carbohydrate moieties are given in the original paper [13] while the charges for the aromatic groups were based on those of the Quanta force field (PARM.PRM) with the necessary modifications to obtain neutral fragments. Dihedral constraints on the ν_i pyranosyl puckering angles were required to maintain $^4C_1$ ring form. At each step, the geometry was optimized with the conjugate gradient minimization algorithm until the root-mean-square (rms) gradient was less than 0.001 kcal/(mol Å^2). Non-bonded interactions were evaluated on a group-to-group basis with the groups corresponding to electrostatically neutral fragments. No cutoff for long-range non-bonded interactions was introduced in the calculations.

Restrained MD simulations were performed for various optimized structures of **1** and **2**. Newton's equations of motion were integrated for each atom using the two-step velocity Verlet algorithm [16] implemented in the CHARMm program. All hydrogen atoms were explicitly included although bond lengths involving hydrogens were kept fixed throughout the simulations using the constraint algorithm SHAKE [17]. The trajectories were thermalized by increasing the temperature by 20 K in 1 ps intervals by a velocity reassignment procedure until the desired value of 300 K was obtained, resulting in a heating period of 15 ps. The heating period was followed by an equilibration period of 30 ps, where atomic velocities were scaled if the temperature deviated from the desired value by more than ±5 K. Following the thermalization period the molecular system was allowed to evolve without further interference for subsequent steps of 200 ps. Energy was well-conserved in the simulations, with the average rms fluctuations in the Hamiltonian divided by those of the kinetic energy being less than 4 kcal/mol when collected in 0.1 ps intervals of the production dynamics trajectories. The rms fluctuations in the temperature were about 10 °C.

Calculation of NMR parameters.—Coupling constants, $^3J_{H,H}$, for vicinal hydrogen atoms of a H–C–C–H segment were calculated using a Karplus type equation with the Haasnoot–Altona parametrization [18]:

$$^3J_{H,H} = P_1\cos^2(\Theta) + P_2\cos(\Theta) + P_3 + \sum\Delta\chi_i\left(P_4 + P_5\cos^2\left(\xi_i\Theta + P_6|\Delta\chi_i|\right)\right). \quad (1)$$

It accounts for J dependence on the dihedral angle (Θ) of the H–C–C–H fragment, on the electronegativity of participating atoms [19] and on the orientation of the α and β substituents. The heteronuclear coupling constant $^3J_{H,C}$ across the glycosidic linkage was calculated by using the equation for the C–O–C–H segment proposed by Tvaroska et al. [20]:

$$^3J_{H,C} = 5.7\cos^2(\Theta_H) - 0.6\cos(\Theta_H) + 0.5. \quad (2)$$

In the simulation of relaxation data of flexible carbohydrate systems internal dynamics must be accounted for by using appropriate expressions for the spectral densities [$J(\omega)$] associated with ensemble-average internuclear distance matrices ($\langle r^{-6}\rangle$ and $\langle r^{-3}\rangle$). Thus, theoretical carbon T_1 and NOE data have been established with the 'model-free' formalism [21], in which a physical motional model can be described with only three parameters, S^2, τ_c, and τ_e (S^2, the spatial restriction of internal motion, which is equal to 1 for a rigid molecule and to 0 for a totally-flexible molecule; τ_c, the correlation time for overall reorientation; and τ_e, the correlation time for internal motion). NOESY volumes were obtained by back calculation of the relaxation matrix established with the dynamic model derived from the carbon relaxation data and the MD interproton distance matrices as previously described [22,23].

3. Results and discussion

As reported in prior work [4], numerous sets of glucosyl signals were detected in the 400 MHz (100 MHz) ^{1}H (^{13}C) spectrum of **1** in acetone-d_6 and inspection of both ^{1}H and ^{13}C resonances revealed several unusually broad signals suggesting that the C_1 form of β-CD **1** was also undergoing some form of chemical exchange. The following strategy was adopted to elucidate the nature of these various dynamic processus: (1) assignment of the ^{1}H and ^{13}C chemical shifts based on 2D correlation and NOESY spectra, (2) determination of the macrocylic puckering of both the C_1 and C_7 conformers through the experimental interglycosidic heteronuclear scalar coupling constants and homonuclear NOEs, (3) detection of chemical exchange through variable-temperature spectra, (4) estimation of the amplitude of fast internal motion (pico- to nanosecond timescale) from

laboratory-frame heteronuclear relaxation data, and finally (5) exploration of nanosecond fluctuations in macrocyclic puckering with molecular modeling.

NMR Chemical shift assignment and coupling constant data.—The anomeric region of the 100.6 MHz inverse-gated ^{13}C spectrum of **1** contained seven resonances of equal intensity and one remaining signal which integrated for twice that of the others. Hereafter, these conformers will be referred to as **1A** (the asymmetric C_1 form) and **1S** (the C_7 conformer). The glucosyl residues of **1A** were labeled 1 to 7 in the order of decreasing chemical shifts for the signals of the anomeric carbons. A heteronuclear correlation spectrum led to assignment of the eight anomeric protons which were labeled H-1(1) to H-1(7) for **1A** and H-1(S) for **1S**. Favorable spectral dispersion allowed complete assignment of the H-1 to H-5 signals of both **1A** and **1S** conformers. The primary hydroxyl proton resonances of **1S** and those of six of the seven residues of **1A** were identified in a long-range COSY experiment. The remaining glucosyl methylene signals, which had been unambiguously detected in the HETCOR experiment, were assigned to H-6a(3) and H-6b(3) (by convention, H-6a refers to the methylene proton which resonates at lower field). The ^{1}H and ^{13}C chemical shift data for the glucosyl residues of **1A** and **1S** are collected in Tables 1 and 2.

Several of the multiplets for H-1 (**1S** and residues 5 and 7 of **1A**), H-2 (**1S** and residue 1 of **1A**), and H-3 (residues 6 and 7 of **1A**) were located in non-overlapping regions of the 400.13 MHz 1D spectrum and therefore the corresponding $^{3}J_{1,2}$ and $^{3}J_{2,3}$ coupling constants could be determined very precisely (± 0.1 Hz/pt). Comparison of the fine structure of the eight H-1/H-2 cross-peaks in the expanded region of the COSYDQF spectrum indicated that all of the vicinal coupling constants for these two spins in both the **1A** and **1S** conformers were almost identical. Similarly, inspection of the eight crosspeaks for H-3/H-4 of **1A** and **1S** reveals analogous $^{3}J_{3,4}$ and $^{3}J_{4,5}$ coupling constant patterns. Upon examining the fine structure of the H-4/H-5 cross-peaks (H-5 in F2), it was evident that four sets of peaks were very similar

Table 2
100.6 MHz ^{13}C chemical shifts of a 10 mM solution of **1** in acetone-d_6 referenced to the solvent methyl signal (δ_C 28.1 ppm)

Sugar	C-1	C-2	C-3	C-4	C-5	C-6
1	100.50	77.35	78.88	80.90 [a]	68.97	62.72
2	98.37	79.21	79.66	83.11 [a]	70.59	64.97
3	97.50	78.00 *	78.14	80.71 [c] *	70.53	62.95
4	97.32	79.35	80.80	72.01 *	67.94	63.54
5	96.82	78.48	80.07 [c]	79.49	69.60	65.33
6	94.95	79.49	79.74 [b]	73.84	66.42	66.64
7	94.75	77.79	81.38 [b]	83.23	67.94	63.20
Sym	97.71	78.14	79.79	78.27	69.74	63.25

[abc] Carbon assignments may be reversed.
* Coalescence-broadened resonances.

Table 1
400 MHz ^{1}H chemical shifts (multiplicity, coupling constants) [a] of a 10 mM solution of **1** in acetone-d_6 referenced to the residual solvent signal (δ_H 2.2 ppm)

Sugar	H-1	H-2	H-3	H-4	H-5	H-6a	H-6b
1	5.336 [a] (d, 3.2)	3.603 (dd, 9.5–3.2)	3.70 [b] (t, g)	4.12 (t, g)	4.49 (d, g)	5.10 (d, tg)	4.98 (tg)
2	5.509 (d, 2.5)	3.95 (dd, g, p)	4.88 (t, g)	4.07 (t, g)	5.23 (t, tg)	5.69 (d, 11.6)	4.69 (t, tg)
3	6.244 (d, p)	4.057 (dd, 9.9, 3.2)	5.10 (t, g)	4.65 (t, g)	4.65 AB	4.99 (d, tg)	4.78 (d, tg)
4	5.173 (d, 3.4)	3.666 (dd, 9.4, 3.2)	3.75 (t, g)	4.38 (t, g)	3.98 (d, g)	5.53 (d, tg)	5.16 (d, tg)
5	5.598 (d, 3.4)	3.921 (dd, g, p)	4.65 (t, g)	4.74 (t, 9.5)	5.47 (d, g)	6.06 (d, 13.1)	5.92 (d,13.1)
6	5.474 (d, 2.5)	3.141 (dd, g, p)	4.21 (t,9.5)	3.91 (t, g)	4.99 (d, g)	5.47 (d, g)	4.48 (d, g)
7	5.959 (d, 3.4)	3.702 (dd, 9.5, 3.2)	4.22 (t, 9.5)	4.14 (t, g)	4.85 (d, tg)	5.28 ABX	5.22 ABX
Sym	5.617 (d, 3.4)	3.863 (dd, 9.1, 3.2)	4.47 (t,g)	4.38 (t,g)	4.68 (d, g)	5.13 ABX	5.13 ABX

[a] Key: p = 0–4 Hz; g ~ 8 Hz; tg > 11 Hz; d = doublet; t = triplet.

(**1S** and residues 1, 5, and 4 of **1A**). In contrast, the F2 width of the H-4/H-5 crosspeaks of residues 2 and 6 of **1A** were almost twice as large indicating that the summed $^3J_{5,6a}$, and $^3J_{5,6b}$ value was much larger. The F2 width of H-4/H-5 was intermediate in the case of residue 7, whereas H-4/H-5 crosspeaks were not detected for residue 3. These rough estimates of the H-5/H-6 coupling constants along with those that could be measured in the 1D spectrum [the signals for H-6a(5) and H-6b(5) were clearly visible] are also collected in Table 1.

Pyranosyl ring conformation.—The most common ring form for the α-glucopyranosyl residues of CDs is $^4C_1$. However, the guest-induced conformational change to the $^0S_2$ form has been reported for the crystal structure of heptakis(2,3,6-tri-*O*-methyl)-β-cyclodextrin complexes of *m*-iodophenol and 4-biphenylacidic acid [24]. Theoretical values for the vicinal coupling constants of the $^0S_2$ form as well as the neighbouring $B_{2,5}$ and $^{0,3}B$ forms on the pseudorotational wheel were reported [25] for an α-glucosyl residue substituted by a nitrilium ion at C-1. The $^3J_{1,2}$ and $^3J_{2,3}$ coupling constants for all three conformers are very different (0.9 and 3.8, 7.1 and 2.9, and 7.1 and 0.5 Hz for $B_{2,5}$, $^{0,3}B$, and $^0S_2$, respectively) from those of both **1A** and **1S** which are analogous to the values calculated [26] for the $^4C_1$ form of α-glucopyranose (3.6 and 9.7 Hz) indicating that both conformers of modified β-CD **1** adopted the latter pyranosyl ring form.

Rotamer distribution.—The $^3J_{5,6a}$ and $^3J_{5,6b}$ values for the ideally staggered GG, GT, and TG rotamers [27] are very different (1.1 and 2.9, 4.9 and 10.8, and 10.8 and 3.1 Hz, respectively, for GG, GT, and TG) and these parameters are an excellent probe of the conformation of the exocyclic group. In a conformational study of hydroxymethyl groups in carbohydrates, Bock and Duus [28] showed that the populations of GG and GT rotamers of α-glucosyl sugars are generally roughly 1:1 with a negligible population of the TG orientation. As regards CDs, the major rotamer in solution adopts the GG orientation [29]. In a study of β-CD dodecahydrate [30] and in the aforementioned study of crystalline inclusion complexes [24], five of the residues presented the GG conformation while the remaining two adopted GT geometry. From the description of the fine structure of the H-5 multiplets it could be deduced that the primary hydroxyl substituents of **1S** and residues 1, 5, and 4 of **1A** adopt the GG conformation, whereas those of residues 2 and 6 present the GT orientation.

Sequential information.—The 400.13 MHz phase-sensitive NOESY spectrum corroborated the $^4C_1$ conformation of the pyranosyl rings of **1A** and **1S**. Strong crosspeaks for the H-1/H-2 and H-2/H-4 interactions were detected for all eight sugars. Partial sequential information for **1A** could be deduced from the H-1/H-4′ crosspeaks. However, a two-fold variation in concentration between the samples used for the COSYDQF and NOESY experiments led to significant shifts in the certain resonance frequencies [for example, the signals of H-3(6) and H-3(7) became superposed] and as a result the chemical shifts of H-4(1) and H-4(7) (4.12 and 4.14 ppm, respectively, in the sample used for the COSYDQF spectrum) could no longer be distinguished at 400.13 MHz. At this magnetic field strength, both **–1–2–7–6–5–3–4–** and **–2–1–7–6–5–3–4–** sequences were compatible with data for **1A**. The 750.13 MHz NOESY spectrum of **1** is given in Fig. 2. Unambiguous assignment of the H-1/H-4′ crosspeaks was possible due to the greatly-improved signal dispersion and signal-to-noise ratio and the sequence for **1A** was shown to be **–1–2–7–6–5–3–4–** (Fig. 3). Moreover, crosspeaks between both H-2 and H-3 and the two methylene protons of the corresponding benzyl substituents were clearly visible. Thus, all of the benzyl methylene spins were assigned and these ^{1}H and ^{13}C chemical shift data are collected in Table 3.

Glycosidic linkage.—Heteronuclear coupling constants across the glycosidic bond were measured with the ^{13}C-ω_1-half-filtered NOESY [11] which is based on proton-detection of $^3J_{C,H}$ coupling constants via E. COSY [31] type cross-peak patterns and can be applied to samples of relatively low concentration (~ 20 mM). The related ^{13}C-ω_1-half-filtered ROESY [32] technique was reported in a study of cyclic glucosyl oligomers. The expanded region containing the H-1(4)/H-4(1) crosspeaks is given in Fig. 4 and the heteronuclear coupling constant data are collected in Table 4. It can be seen that the average values of $^3J_{C\text{-}1,H\text{-}4'}$ and $^3J_{H\text{-}1,C\text{-}4'}$ for **1A** are very different from those of **1S** suggesting very different conformations of the macrocycle. The relative signs of the coupling constants are also determined with this method [for example, the opposite tilt is observed for the geminal H-1(4)/C-2(4) crosspeaks above indicating a negative coupling constant] which would be useful for deriving Karplus-type equations.

Normalized $a_{H\text{-}1,H\text{-}4'}$ crosspeak volumes are collected in Table 4. The average intensity of the **1A** interglycosidic crosspeaks (0.032) is slightly greater than that of the intraresidue $a_{H\text{-}1,H\text{-}2}$ ones (0.020). As the $r_{H\text{-}1,H\text{-}2}$ distance is typically ~ 2.45 Å for α-Glc*p*,

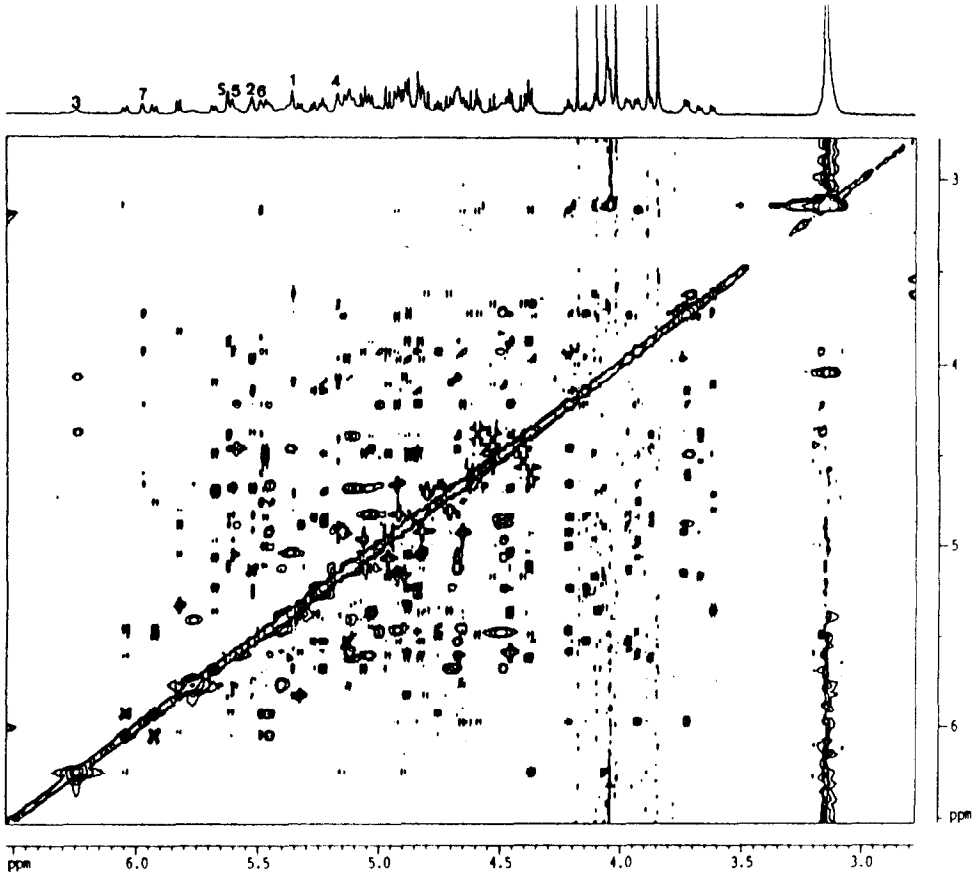

Fig. 2. 750.13 MHz phase-sensitive NOESY spectral region (below) containing the resonances of the sugar protons of a 10 mM sample of modified β-cyclodextrin **1** in acetone-d_6. The corresponding 1D proton spectrum is also given (above).

this indicates that the corresponding average distance $r_{H\text{-}1,H\text{-}4'}$ must be fairly short. The $a_{H\text{-}1,H\text{-}4'}$ values are fairly homogeneous (0.037 ± 0.005) with the exception of two very weak interactions between Glc(3)/Glc(4) and Glc(4)/Glc(1) (and thus two longer $r_{H\text{-}1,H\text{-}4'}$ distances) corroborating a C_1 conformation for the **1A** macrocycle.

A third criteria for evaluating the orientation of the glycosidic linkages was the carbon chemical shifts of C-1 and C-4′. It is known that significant variations in ^{13}C chemical shifts of carbohydrates are caused by spatial proton–proton interactions, which induce a polarization of the C–H bonds and, as a result, a change in the shielding of the carbon nuclei [33]. Correlation of these chemical shift variations, $\Delta\delta_C$,

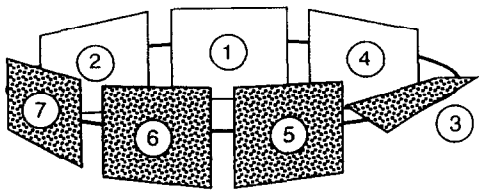

Fig. 3. Schematic representation of the sugar cyclodextrin backbone in **1A** as deduced from NMR experiments. View from above the primary face.

Table 3
^1H and ^{13}C NMR data [a] of the benzyl methylene carbons of a 10 mM solution of **1**

	δ_C	δ_{Ha}	δ_{Hb}	$^2J_{Ha,Hb}$
Cb-3(5)	75.52	5.445	4.90	d, tg
Cb-3(6 or 7)	75.06	5.574	4.458	d, tg
Cb-3(3)	74.88 *	5.750	5.389	9.6
Cb-3(2)	74.74	5.80	5.305	11.0
Cb-3(1)	74.46	4.859	4.463	d, tg
Cb-3(S)	74.36	5.352	5.015	11.0
Cb-2(3)	73.70 *	5.150	4.866	d, tg
Cb-3(4)	73.18	5.137	4.911	d, tg
Cb-3(6 or 7)	72.62	4.900	4.634	d, tg
Cb-2(5)	71.71	5.036	4.929	d, tg
Cb-2(S)	71.67	4.858	4.798	d, tg
Cb-2(7)	71.48	4.602	4.554	d, tg
Cb-2(2)	71.45	4.882	4.784	d, tg
Cb-2(1)	71.30	4.784	4.676	d, tg
Cb-2(6)	71.30	4.563	4.340	d, tg
Cb-2(4)	71.02	4.518	4.382	d, tg

[a] Conditions and symbols as in Tables 1 and 2.

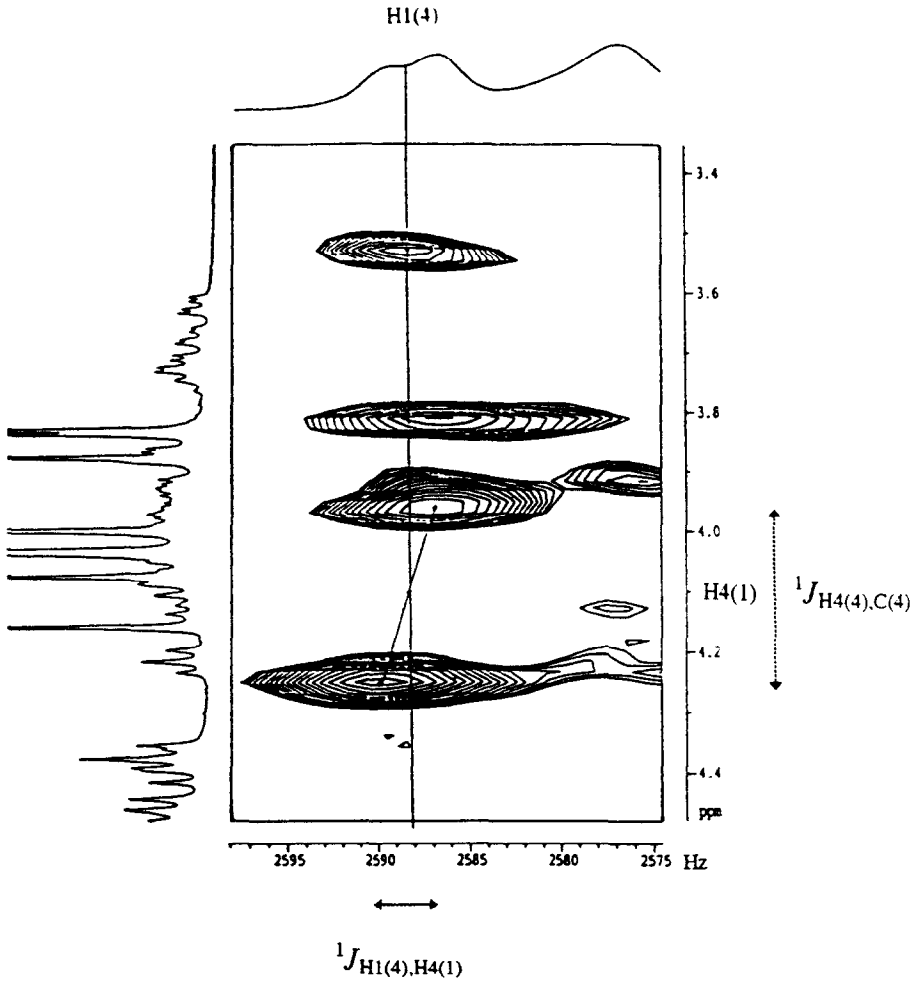

Fig. 4. Region of the 500.13 MHz ^{13}C-ω_1-half-filtered NOESY spectrum containing the H-1(4)/H-4(1) crosspeaks of a 20 mM sample of modified β-cyclodextrin **1** in acetone-d_6. The corresponding 1D proton spectrum is also given (above).

with Φ_H and Ψ_H has been reported for solid-state ^{13}C spectra [34]. Bock et al. [35] have shown that in the case of non-reducing α-(1 → 4)-linked glucopyranose residues in oligosaccharides, $\Delta\delta_{C\text{-}1}$ and $\Delta\delta_{C\text{-}4}$ (i.e. $\Delta\delta_{C\text{-}1} = \delta_{obs} - \delta_{ref}$, where δ_{ref} is the chemical shift of unsubstituted α-Glc*p* [36]) can be correlated to the Ψ_H value or alternatively the $r_{H\text{-}1,H\text{-}4'}$ distance. Accordingly, $r_{H\text{-}1,H\text{-}4'}$ values were evaluated from the $\Delta\delta$ values of C-1 and C-4′ of **1A** and the fitting parameters reported previously [36]. In the case of the 3 → 4 glycosidic linkage fairly long $r_{H\text{-}1,H\text{-}4'}$ distances were obtained from C-1(3) (2.60 Å) and C-4(4) (2.85 Å) $\Delta\delta$ values in agreement with the quantitative NOESY volumes. However, much poorer agreement between the $\Delta\delta_{C\text{-}1}$ and $\Delta\delta_{C\text{-}4}$ estimations of $r_{H\text{-}1,H\text{-}4'}$ was obtained for the remaining linkages suggesting that other effects were also important.

Slow conformational exchange.—Certain signals in the ^{1}H and ^{13}C spectrum were very broad suggesting that the corresponding spins were undergoing chemical exchange. The 100.6 MHz ^{13}C spectra of **1** are given in Fig. 5. Coalescence of C-2(3), C-4(3), C-4(4), Cb-2(3) and Cb-3(3) was observed at 296 K and these signals narrowed significantly at 323 K. This phenomenon, which is localized at residue 3 (similarly, in the ^{1}H spectrum, the H-1(3) signal is the only anomeric resonance which does not show splitting for the H-1/H-2 coupling), suggesting that this sugar can adopt at least two different stable C_1 conformations at room temperature.

Dynamic model.—In order to establish a dynamic model for fast (nanosecond timescale) conformational fluctuations, ^{13}C T_1 and NOE factors (η) were measured and these data are collected in Tables 5 and 6 along with the experimental deviations. The average standard deviation obtained with the fitting routine for the T_1 values is also indicated. The average T_1 value for both **1S** and **1A** conformers was 0.19 s. In the case of **1A** those of the linkage carbons were slightly lower (C-1 and C-4, 0.16 and 0.18 s, respectively).

Theoretical plots of carbon $1/T_1$ as a function of

Table 4
Theoretical and experimental inter-residue heteronuclear coupling constants, and NOESY crosspeak volumes (internuclear distances, $r_{H\text{-}1,H\text{-}4'}$) of β-CDs **1** and **2**

		Simulated data			Experimental data		
		$^3J_{H\text{-}1,C\text{-}4'}$ (Hz) (Φ_H (°)) [a]	$^3J_{C\text{-}1,H\text{-}4'}$ (Hz) (Ψ_H (°)) [a]	$r_{H\text{-}1,H\text{-}4'}$ (Å)	$^3J_{H\text{-}1,C\text{-}4'}$ (Hz) (Φ_H (°)) [a]	$^3J_{C\text{-}1,H\text{-}4'}$ (Hz) (Ψ_H (°)) [a]	$a_{H\text{-}1,H\text{-}4'}$ ($r_{H\text{-}1,H\text{-}4'}$ (Å))
1S		5.4 (10.3 ± 11.5)	1.3 (28.2 ± 17.7)	2.52 ± 0.14	1.5	2.0	0.032
1A	1	5.2 (15.7 ± 13.9)	4.4 (28.2 ± 17.7)	2.30	2.5	3.5	0.035
	2	5.3 (13.1 ± 13.6)	5.2 (16.6 ± 15.3)	2.24	3.0	4.5	0.037
	3	4.5 (26.3 ± 17.2)	0.8 (73.3 ± 16.2)	2.78	0	1.5 [b]	0.017
	4	4.0 (32.9 ± 16.3)	4.1 (32.2 ± 20.4)	2.74	3.0	4.0 [c]	0.017
	5	4.2 (31.1 + 12.4)	4.6 (24.7 ± 12.7)	2.23	4.0	0	0.039
	6	5.5 (9.2 ± 13.8)	4.9 (21.3 ± 14.3)	2.24	3.5	–	0.037
	7	5.3 (14.3 ± 13.8)	5.4 (11.5 ± 14.8)	2.15	2.0	–	0.042
β-CD (X-ray structure)					(7.2)	(12.1)	(2.09)
β-CD (solution)					5.7	5.6	
2		4.0 (33.1 ± 8.1)	4.7 (24.6 ± 10.5)	2.41 ± 0.13			

[a] Absolute values.
[b] Values very poorly defined.
[c] Values poorly defined.

τ_c are given in Fig. 6a. The two values for S^2 (0.9, left; 0.7, right) which have been used to establish these curves cover the range of order parameters which have been obtained by fitting of experimental data [22,23,37–41]. Several correlation times, covering three orders of magnitude, for the internal dynamics (τ_e: key) have been considered. Two conclusions can be drawn from these plots. The T_1 values of **1A** and **1S** correspond to the flat region of the $1/T_1$ vs τ_c plot and therefore molecular reorientation is not well-defined from these data. Correlations times in the range of 0.6–2.6 ns associated with appropriate values of τ_e would all be compatible with the experimental data. Secondly, from the curves in Fig. 6a, it can be seen that it is not possible to distinguish between the case of low-amplitude fluctuations ($S^2 = 0.9$) associated with various τ_e values and less restricted internal dynamics ($S^2 = 0.7$) associated with fairly slow (200–800 ps) internal motion.

The NOE factors were less uniform (0.45–0.74) with average $\eta_{C\text{-}1}$ and $\eta_{C\text{-}x}$ ($x = 2$–5) values of 0.51 and 0.64 for **1A**. The $\eta_{C\text{-}1}$ value of **1S** (0.47) was slightly lower. Inhomogeneous carbon T_1 and η data can be an indication of anisotropic overall tumbling. However, the overall shape of **1A** is very close to that of a sphere of radius 10–11 Å (the diameter parallel to the cavity is roughly 20–22 Å while the diameter perpendicular to the cavity is 20–22 Å) precluding anisotropic overall motion (Fig. 7). Inspection of the η curves (Fig. 6b) shows that this parameter is not affected by internal dynamics when the motion is very restricted ($S^2 = 0.9$). Thus, the wide range of experimental η values which were obtained for **1A** cannot be reproduced for a model with spatially restricted internal motion. On the contrary, η is very sensitive to internal motion of sufficient amplitude ($S^2 < 0.8$) for τ_c values greater than 0.5 ns. The motional model which emerged from the carbon relaxation data was characterized by an order parameter of 0.76, typical of pyranosyl carbons [22,23,38], a correlation time for internal motion of ~0.4 ns in agreement with values reported for carbohydrates [22,23], and a τ_c value between 0.8–1.0 ns in agreement with hydrodynamic theory. This dynamic repre-

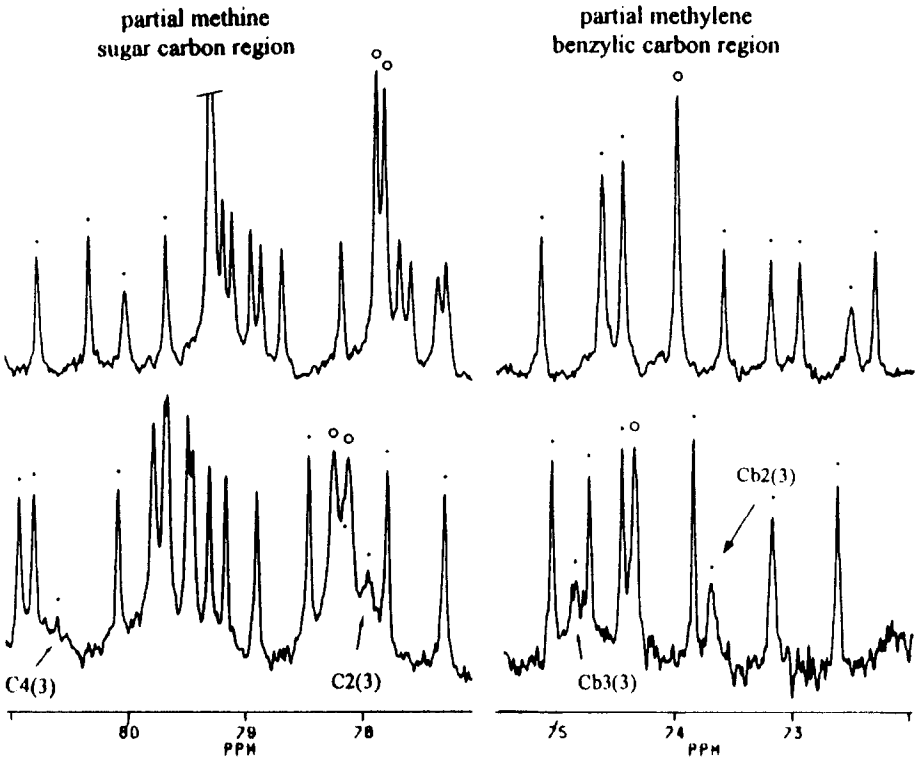

Fig. 5. 100.6 MHz carbon spectra of a 10 mM sample of modified β-cyclodextrin **1** in acetone-d_6 at 296 K (below) and 323 K (above). Signals for C-2(3), C-4(3), Cb-2(3) and Cb-3(3) have been labeled. Open circles (○) and dots (●) indicate signals of **1S** and **1A**, respectively.

sentation is very different from the one established for **2** based on carbon relaxation data [41] which corresponded to a very rigid structure. However, the relative rigidity of β-CDs is generally attributed to inter-residue H-bonding and therefore a difference in the motional models of **1** and **2** is not entirely surprising.

Molecular modeling.—The initial coordinates for the various β-CD models were those reported in the neutron and X-ray diffraction study of β-cyclodextrin ethanol octahydrate [15]. The glycosidic torsional angles are all located in the same low-energy region (Φ_H, −14 to 3°; and Ψ_H, −12 to 21°; B-well of the maltose Φ_H, Ψ_H map [42,43]). Six out of seven exocyclic groups presented the GG orientation while the remaining one adopted the GT conformation. The values of the glycosidic valence angles, C-1–O-4′–C-4′ (β), were between 119–147° and the macrocyclic puckering angles, θ_L (O-4–C-4–C-1–O-4′), varied from −4 to +6°. The average value of the $r_{H\text{-}1,H_6 4'}$ distance across the glycosidic linkages was 2.09 Å. Upon relaxation of **2** in the HGFB force field, the average values of Φ_H (−5°) and Ψ_H (−2°) increased and decreased, respectively, while the average $r_{H\text{-}1,H\text{-}4'}$ distance increased from 2.09 to 2.25 Å. The average β glycosidic valence angle was 118° in good agreement with the value calculated for 2-methoxytetrahydropyran in an ab initio study [44].

During the molecular dynamics simulations of **2** with the HGFB force field (a total of 200 ps) the average fluctuations of the Φ_H, Ψ_H dihedral angles were ~ 10°. The average value of the macrocyclic puckering dihedral θ_L was 4.3°. Although the corresponding low-energy regions were reasonably well-explored during these trajectories, transitions to neighbouring wells did not occur. In a study of maltose, similar behavior was observed for the 80-ps trajectories (CHARMM) in vacuum and in aqueous solution [45]. In contrast, a broad distribution of Φ_H, Ψ_H values encompassing the whole A–C low-energy region was reported for 100 ps MD simulations of **2** in vacuo and in water with the GROMOS force field [46]. The average values of the theoretical heteronuclear $^3J_{H\text{-}1,C\text{-}4'}$ and $^3J_{C\text{-}1,H\text{-}4'}$ coupling constants from the present MD simulation are analogous (5.4 and 4.4 Hz) to the corresponding experimental values (5.7 and 5.6 Hz) reported by Mulloy et al. [47].

MD simulations of modified β-CD **1S** were performed with harmonic constraints on both ν_i (pyranosyl puckering dihedrals) and five of the seven

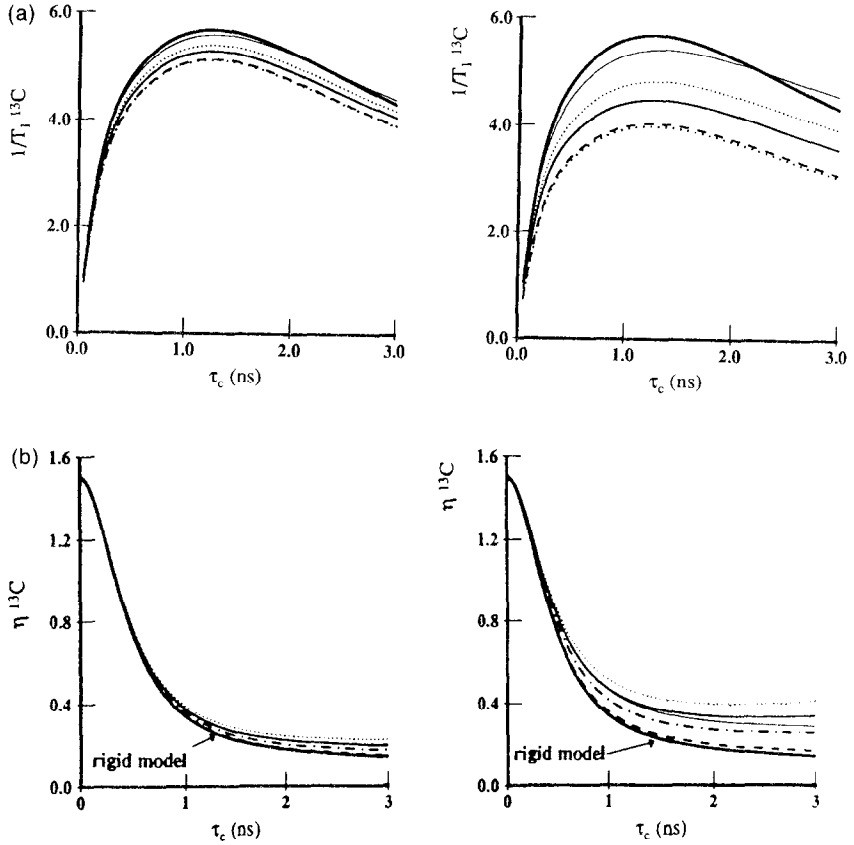

Fig. 6. (a) 100.6 MHz theoretical carbon longitudinal relaxation rates, $1/T_1$, as a function of molecular correlation time, τ_c, established with the model-free spectral densities for S^2 values of 0.9 (left) and 0.7 (right). The upper boldface trace corresponds to a rigid molecule, whereas the remaining traces correspond to a flexible one (key for the τ_c values in ps: 1, dotted; 10, dashed; 100, solid; 200, small dots; 800, narrow solid). (b) 100.6 MHz theoretical carbon heteronuclear NOE factor, η, as a function of molecular correlation time, τ_c, established with the model-free spectral densities. The key is the same as in (a). The trace for a rigid molecule is also given (lowest curve).

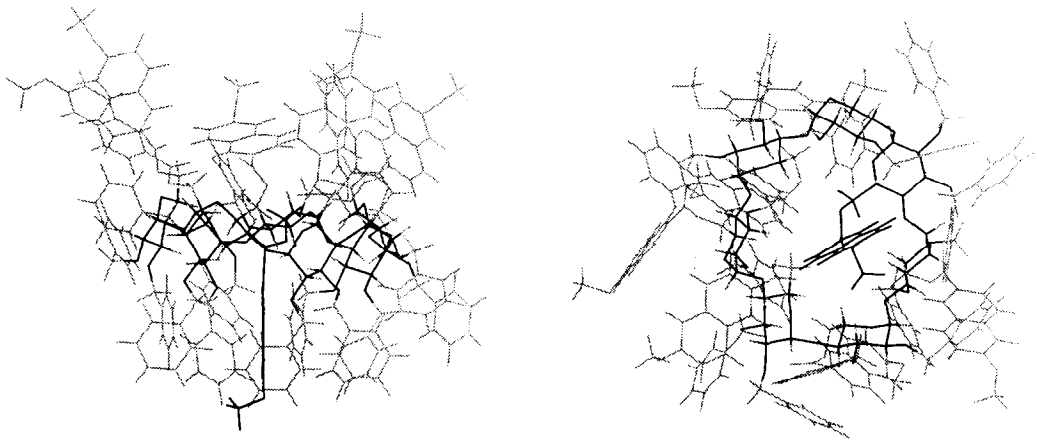

Fig. 7. Low-energy C_1 conformer of modified β-cyclodextrin **1** view from above (right) and from the side (left).

ω torsional angles (in agreement with the available NMR data). The average values for the seven Φ_H and Ψ_H dihedral angles and for the $r_{H\text{-}1,H\text{-}4'}$ distances during a nanosecond MD trajectory are collected in Table 4. One of the Φ_H, Ψ_H pairs was located in the A-well, two were situated in the B-well while the four others occupied the D-well [43]. The average fluctuations of these dihedral angles were $\sim 15°$ and during these trajectories no transitions to neighbouring wells occurred. The average proton interglycosidic distance of the MD trajectories increased from 2.41 to 2.52 Å upon converting **2** to **1S**. The latter value is in reasonable agreement with the average $a_{H\text{-}1,H\text{-}4'}$ crosspeak volume of **1S**, 0.032 ± 0.005 (the average $a_{H\text{-}1,H\text{-}2}$ value of 0.027 corresponds to an average $r_{H\text{-}1,H\text{-}2}$ of 2.45 Å). In contrast, in comparison to the average absolute Φ_H (61.7°) and Ψ_H (55.3°) values calculated from the heteronuclear coupling constants, the average theoretical Φ_H and Ψ_H dihedrals are much too low (10° and 28°, respectively). The average value of the macrocyclic dihedral θ_L is 4.3°.

The NMR-defined **1A** conformer was obtained from **1S** by first taking into account the vicinal homo- and heteronuclear coupling constant data. Accordingly, the orientations of the naphthoyl group (ω) and the glycosidic linkages (Φ_H, Ψ_H) were varied arbitrarily in order to reproduce the dihedral angles in Table 1 (ω) and 4 (Φ_H, Ψ_H), respectively. It should be pointed out that the Karplus-type equation for the H–C–O–C fragment [20] generally has four solutions. From the potential energy maps established for the α-(1 → 4)-linked glucopyranose residues, it was possible to reduce the number of Φ_H values to two ($-90° < \Phi_H < 90°$). The choice of Φ_H then limited the range of Ψ_H values compatible with closure of the macrocycle. A dozen starting geometries were constructed and minimized with harmonic constraints applied to the ν_i, Φ_H, and ω (five out of seven) dihedrals.

During the construction of the **1A** conformers the naphthoyl substituent of residue 3 was positioned directly above the β-CD cavity. Rotation about the Φ_H torsional angle in an attempt to attain the Φ_H value ($\sim 90°$) derived from the experimental coupling constant positioned residue 3 parallel to the plane of the macrocycle and pivoted the substituent into the cavity (θ_L (3) = 11°).

MD simulations were performed with harmonic constraints on either (i) ν_i, Φ_i and five of the ω torsional angles (300 ps, initiated with the geometry which reproduces the $^3J_{C,H}$ data) or (ii) ν_i, five of the ω dihedrals and the $r_{H\text{-}1,H\text{-}4'}$ internuclear distances (1

Table 5
Carbon longitudinal relaxation times [a] (seconds) of a 10 mM solution of **1** in acetone-d_6

	Sugar							
	1	2	3	4	5	6	7	S
C-1	**0.18**[5]	**0.16**[5]	**0.17**[5]	**0.14**[5]	**0.16**[5]	**0.15**	**0.17**	**0.21**
	0.01 [a]	0.01	0.02	0.01	0.01	0.02	0.01	0.01
	(0.07) [b]	(0.08)	(0.06)	(0.07)	(0.08)	(0.06)	(0.07)	(0.03)
C-2	**0.19**	**0.18**		**0.21**	**0.18**[5]	**0.21**	**0.19**[5]	**0.18**
	0.02	0.00		0.01	0.02	0.01	0.02	0.02
	(0.05)	(0.08)		(0.04)	(0.06)	(0.04)	(0.05)	(0.05)
C-3	**0.17**[5]	**0.18**[5]	**0.17**[5]	**0.17**[5]	**0.20**	**0.18**[5]	**0.17**	**0.19**
	0.02	0.01	0.01	0.05	0.00	0.01	0.01	0.03
	(0.05)	(0.04)	(0.05)	(0.07)	(0.05)	(0.04)	(0.06)	(0.06)
C-4	**0.17**	**0.19**			**0.19**[5]	**0.18**[5]	**0.16**[5]	**0.17**
	0.00	0.01			0.01	0.02	0.01	0.01
	(0.06)	(0.06)			(0.06)	(0.05)	(0.05)	(0.05)
C-5	**0.18**[5]	**0.18**	**0.17**[5]	**0.19**[5]	**0.18**[5]	**0.15**	**0.19**[5]	**0.19**
	0.01	0.01	0.02	0.02	0.01	0.00	0.02	0.00
	0.07	(0.04)		(0.04)	(0.07)	(0.09)	(0.04)	(0.03)
C-6	**0.08**[5]	**0.08**	**0.09**[5]	**0.08**[5]	**0.10**[5]	**0.09**	**0.09**	**0.09**
	0.01	0.02	0.01	0.01	0.02	0.01	0.00	0.00
	(0.07)	(0.08)	(0.07)	(0.09)	(0.06)	(0.09)	(0.04)	(0.04)

[a] Key: average values for two experiments are in boldface, the deviation between the two experimental values is given below in plain font and the standard deviation of the fitting routine is indicated in parentheses.

Table 6
100.6 MHz ^{13}C heteronuclear nuclear Overhauser factors [a], η, of a 10 mM solution of **1** in acetone-d_6

	Sugar							
	1	2	3	4	5	6	7	S
C-1	0.45	0.50	0.53	0.53	0.63	0.63	0.47	0.46
	(0.07)	(0.07)	(0.05)	(0.05)	(0.03)	(0.03)	(0.05)	(0.04)
C-2	0.72							
	(0.07)							
C-3	0.70						0.51	
	(0.08)						(0.03)	
C-4		0.58					0.58	
		(0.09)					(0.09)	
C-5	0.74	0.62	0.62	0.60			0.60	
	(0.09)	(0.07)	(0.07)	(0.05)			(0.05)	
C-6		0.47			0.50			
		(0.06)			(0.05)			

[a] Key: experimental values are the average of four measurements; the standard deviations are indicated in parentheses.

ns, initiated with the geometry which reproduces $a_{H\text{-}1,H\text{-}4'}$ crosspeak volumes). In the first trajectory, the average $r_{H\text{-}1,H\text{-}4'}$ internuclear distance was much too long (> 2.8 Å) and the Φ_H, Ψ_H dihedrals did not retain the values derived from the heteronuclear interglycosidic coupling constants; an abrupt transition of one of the two unconstrained exocyclic dihedrals, $\omega(7)$, from GT to the GG occurred followed by sharp transitions of three Ψ_H angles. One of these angles, which was initially in the D-well, crossed over to the F-well [42,43]. Simultaneously, these transitions, which were associated with a variation in potential energy (−1.5 kcal/mol), produced large variations in the macrocyclic puckering $\Delta\theta_L$ (7°) of four glucosyl residues and in the proton interglycosidic distances (roughly 0.5 Å) for four linkages. This event lead to a stable conformation, which was evaluated to be −4.1 kcal/mol with respect to **1S**, and the resulting dihedrals persisted durably for the remainder of the trajectory.

In the second trajectory (1 ns), the simulation did not correctly reproduce the heteronuclear coupling constant data. The theoretical values were much too high (4.8 and 4.2 Hz for $^3J_{H\text{-}1,C\text{-}4'}$ and $^3J_{C\text{-}1,H\text{-}4'}$, respectively). However, this family of structures was stable in the HGFB force field albeit 15 kcal/mol above the most stable geometry revealed by the conformational searching. The average fluctuations of the Φ_H, Ψ_H dihedrals were ~ 10° and after 600 ps simultaneous transitions of two Φ_H, Ψ_H pairs to neighbouring wells occurred. The dihedrals of these two glycosidic linkages evolved in opposite directions (A → D and D → A) so as to preserve the overall average macrocyclic puckering (θ_L = 5.4°).

Neither type of simulation led to a structure which could reproduce both the interglycosidic NOESY crosspeak volumes and the related heteronuclear coupling constants, but as the NMR data represent a time-averaged structure this was not entirely surprising. It is noteworthy that all the structures which could reproduce the heteronuclear coupling constant data were unstable in the HGFB force field. In contrast, the time-averaged structure from the second type of trajectory, which gave very good agreement with the NOESY data, corresponded to a local minima.

In conclusion throughout a total of close to 2 ns of MD simulations of modified β-CD **1**, two types of interglycosidic transitions were observed, auto-compensated events which did not alter the overall macrocyclic puckering and irreversible events which were accompanied by a net change in the β-CD puckering. The internal motions which modulate the laboratory-frame relaxation data (nanosecond timescale) could well be related to the former fluctuations. In contrast, the best model which emerged from the MD simulations for the transition state of the C_1/C_7 equilibrium was the latter irreversible-type of event.

In a molecular mechanics study of symmetry-breaking in cyclodextrins, energy optimization was performed with both the MM2 and AMBER force fields [48] In the case of β-CDs, the C_1 conformers were shown to be more stable than the C_7 one encouraging the author to postulate that the C_7 NMR representation corresponds to a time-averaged structure. Evolution of the C_7 conformers to C_1 geometries led to an increase in the macrocyclic puckering θ_L (θ_L = O-4–C-4–C-1–O-4′) range which passed from 0 ± 2° to 0 ± 20°. The macrocyclic puckering of all the **1S** and **2** structures reported in the present work belongs to the second category corroborating the conclusions of Lipkowitz.

4. Conclusions

The NMR data clearly indicate that a change in the conformation of the β-CD macrocycle is responsable for the existence of the C_1 conformer of **1**. The ^{13}C-ω_1-half-filtered NOESY sequence was very satisfactory as it afforded most of the interglycosidic vicinal carbon–proton coupling constants for a 20 mM solution of **1A** and **1S**. This represents a 10-fold gain in sensitivity with respect to the selective INEPT experiment which was recommended [49] recently for the determination of long-range ^{13}C, ^{1}H coupling constants. The dynamic model obtained by fitting the ^{13}C relaxation data with the 'model-free' spectral densities, demonstrates that although β-CD **1** is sterically hindered, it remains a fairly flexible molecule. Variable temperature ^{13}C spectra have also indicated that the residue 3 which is perpendicular to the CD torus undergoes a more local conformational equilibrium with coalescence at room temperature. This only affects the benzyl and the methine carbons (Fig. 7) located outside the cavity suggesting that this process is probably related to the tilt of the pyranosyl ring with respect to the macrocycle.

The nanosecond MD simulations were too short to produce the time-averaged C_7 symmetry corresponding to **1S** as only two transitions were observed over a 2-nanosecond period. Moreover, simulations would have to be run on at least the microsecond scale in

order for these large-amplitude transitions to begin to have any statistical significance. Molecular modeling based on the NMR data points to complexation of one of the naphthoyl substituents. The driving force for the **1S** → **1A** transition may well be the favorable interactions of the exocyclic substituents at C-6 with the rest of the molecule (i.e., the hydrophobic cavity of the β-CD or the other substituents) as the variation of this dihedral appears to initiate rearrangement of the macrocycle. Concerted fluctuations of considerable amplitude were required for a significant variation in macrocyclic conformation indicating that the contribution of activation entropy $\Delta S^{\neq\circ}$ associated with this process must be unfavorable. From the heteronuclear coupling constants it appears that the Φ_H, Ψ_H pair of the residue perpendicular to the β-CD torus is located in an isolated secondary energy well (F-well). In the case of **2,** the pathway between the main low-energy region (A–D-wells) and the F-well includes regions about 10 kcal/mol above the global minimum suggesting that the $\Delta H^{\neq\circ}$ associated with this processus must also be unfavorable. As temperatures greater than 100 °C are required in order to begin to observe the coalescence of the signals of the C_1 and C_7 isomers, it is clear that the energy barrier which separates these two forms is very high.

Despite the understanding gained about of the **1A** conformational behaviour, the present investigation does not provide any definitive clue for predicting whether a symmetrically functionalized β-cyclodextrin will exhibit stable C_1 conformers. Indeed, the rate of the C_1 to C_7 exchange appears to be strongly influenced by subtle variations in the substitution pattern and an extensive study would be required to rationalize the effects of structural modifications on the kinetics of this exchange. From a chemist's point of view, the size of the β-CD cavity is of course the main focus and this parameter does not appear to be significantly affected by the exchange phenomenon. It has been recently shown in a MM study of permethylated CDs that the opening on the secondary hydroxyl face is increased by substitution from 12.5 to 14 Å [50]. Analogous values for this opening have been evaluated in the case of **1S** or **1A**.

References

[1] H.-J. Schneider, *Angew. Chem. Int. Ed. Engl.*, 30 (1991) 1417.

[2] H.-J. Schneider, *Chem. Soc. Rev.* (1994) 227.

[3] P. Ellwood, C.M. Spencer, N. Spencer, J.F. Stoddart, and R. Zarzycki, *J. Incl. Phenom.*, 12 (1992) 121–150.

[4] L. Jullien, J. Canceill, L. Lacombe, and J.-M. Lehn, *J. Chem. Soc., Perkin Trans. 2* (1994) 989–1002.

[5] A.E. Ferentz, J. Wiorkiewicz-Kuczera, M. Karplus, and G.L. Verdine, *J. Am. Chem. Soc.*, 115 (1993) 7569–7583.

[6] P.D.J. Grootenhuis, P.A. Kollman, L.C. Groenen, D.N. Reinhoudt, G.J. van Hummel, F. Ugozzoli, and G.D. Andreetti, *J. Am. Chem. Soc.*, 112 (1990) 4165–4176.

[7] IUPAC-IUB, Commission on Biochemical Nomenclature, *Arch. Biochem. Biophys.*, 145 (1971) 405–421.

[8] S. Macura, Y. Huang, D. Suter, and R.R. Ernst, *J. Magn. Reson.*, 43 (1981) 259–281.

[9] D. Neuhaus and M. Williamson, in *The Nuclear Overhauser Effect in Structural and Conformational Analysis*, VCH Publishers, 1989, p. 292.

[10] Y. Inoue, *Ann. Rep. NMR Spectrosc.*, 27 (1993) 59–101.

[11] P. Schmieder, M. Kurz, and H. Kessler, *J. Biomol. NMR*, 1 (1991) 403–420.

[12] D. Marion and K. Wüthrich, *Biochem. Biophys. Res. Commun.*, 113 (1983) 967–974.

[13] S.N. Ha, A. Giammona, M. Field, and J.W. Brady, *Carbohydr. Res.*, 180 (1988) 207–221.

[14] B. Brooks, R. Bruccoleri, B. Olafson, D. States, S. Swaminathan, and M. Karplus, *J. Comput. Chem.*, 4 (1983) 187–217.

[15] T. Steiner, S.A. Mason, and W. Saenger, *J. Am. Chem. Soc.*, 113 (1991) 5676–5687.

[16] L. Verlet, *Phys. Rev.*, 159 (1967) 98–103.

[17] W.F. Van Gunsteren and H.J.C. Berendsen, *Mol. Phys.*, 34 (1977) 1311–1327.

[18] C.A.G. Haasnoot, F.A.A.M. de Leeuw, and C. Altona, *Tetrahedron*, 36 (1980) 2783–2792.

[19] W.J. Moore, in *Physical Chemistry*, Longman (Ed.), Harlow, 1972.

[20] I. Tvaroska, M. Hricovini, and E. Petrakova, *Carbohydr. Res.*, 189 (1989) 359–362.

[21] G. Lipari and A. Szabo, *J. Am. Chem. Soc.*, 104 (1982) 4546–4559.

[22] N. Bouchemal-Chibani, I. Braccini, C. Hervé du Penhoat, and V. Michon, *Int. J. Biol. Macromol.*, 17 (1995) 177–182.

[23] S.B. Engelsen, C. Hervé du Penhoat, and S. Perez, *J. Phys. Chem.*, 99 (1995) 13334–13351.

[24] K. Harata, F. Hirayama, H. Arima, K. Uekama, and T. Miyaji, *J. Chem. Soc., Perkin Trans. 2* (1992) 1159–1166.

[25] I. Braccini, C. Derouet, J. Esnault, C. Hervé du Penhoat, J.-M. Mallet, V. Michon, and P. Sinaÿ, *Carbohydr. Res.*, 246 (1993) 23–41.

[26] C. Altona and C.A.G. Haasnoot, *Org. Magn. Chem.*, 13 (1980) 417–429.

[27] R.H. Marchessault and S. Perez, *Biopolymers*, 18 (1979) 2369–2374.

[28] K. Bock and J.O. Duus, *J. Carbohyr. Chem.*, 13 (1994) 513–543.

[29] D.J. Wood, F.E. Hruska, and W. Saenger, *J. Am.*

Chem. Soc., 99 (1977) 1735–1740.
[30] K. Lindner and W. Saenger, *Carbohydr. Res.*, 99 (1982) 103–115.
[31] C. Griesinger, O.W. Sorensen, and R.R. Ernst, *J. Am. Chem. Soc.*, 107 (1985) 6394–6396.
[32] L. Poppe, W.S. York, and H. van Halbeek, *J. Biomol. NMR*, 3 (1993) 81–9.
[33] D.M. Grant and B.V. Cheney, *J. Am. Chem. Soc.*, 89 (1967) 5315–5318.
[34] H. Saitô, G. Izumi, T. Mamizuka, S. Suzuki, and R. Tabeta, *J. Chem. Soc., Chem. Commun.* (1982) 1386–1388.
[35] K. Bock, A. Brignole, and B.W. Sigurskjold, *J. Chem. Soc., Perkin Trans. 2* (1986) 1711–1713.
[36] K. Bock and H. Thogersen, in *Ann. Rep. NMR Spectrosc.*, Vol. 13, Academic Press, Paris, 1982, p. 41.
[37] M. Hricovini, R.N. Shah, and J.P. Carver, *Biochemistry*, 31 (1992) 10018–10023.
[38] H. Kovacs, S. Bagley, and J. Kowalewski, *J. Magn. Reson.*, 85 (1989) 530–541.
[39] A. Ejchart and J. Dabrowski, *Magn. Reson. Chem.*, 30 (1992) S115–S124.
[40] D.C. McCain and J.L. Markley, *J. Am. Chem. Soc.*, 108 (1986) 4259–4264.
[41] J. Kowalewski and G. Widmalm, *J. Phys. Chem.*, 98 (1994) 28–34.
[42] S. Ha, L.J. Madsen, and J.W. Brady, *Biopolymers*, 27 (1988) 1927–1952.
[43] V. Tran, A. Buleon, A. Imberty, and S. Perez, *Biopolymers*, 28 (1989) 679–690.
[44] I. Tvaroska and J.P. Carver, *J. Phys. Chem.*, 98 (1994) 9477–9485.
[45] J.W. Brady and R.K. Schmidt, *J. Phys. Chem.*, 97 (1993) 958–966.
[46] M. Prabhakaran, *Biochem. Biophys. Res. Commun.*, 178 (1991) 192–197.
[47] B. Mulloy, T.A. Frenkiel, and D.B. Davies, *Carbohydr. Res.*, 184 (1988) 39–46.
[48] K.B. Lipkowitz, *J. Org. Chem.*, 56 (1991) 6357–6367.
[49] P. Ladam, J. Gharbi-Benarous, M. Piotto, M. Delaforge, and J.P. Girault, *Magn. Reson. Chem.*, 32 (1994) 1–7.
[50] R. Reinhardt, M. Richter, and P.P. Mager, *Carbohydr. Res.*, 291 (1996) 1–9.